Investigation of dielectric barrier discharge dependence on permittivity of barrier materials

Ruixing Li, Qing Tang, Shu Yin, and Tsugio Sato

Citation: Applied Physics Letters **90**, 131502 (2007); doi: 10.1063/1.2716848
View online: http://dx.doi.org/10.1063/1.2716848
View Table of Contents: http://scitation.aip.org/content/aip/journal/apl/90/13?ver=pdfcov
Published by the AIP Publishing

Investigation of dielectric barrier discharge dependence on permittivity of barrier materials

Ruixing Li,[a] Qing Tang,[b] Shu Yin, and Tsugio Sato
Institute of Multidisciplinary Research for Advanced Materials, Tohoku University, Sendai 980-8577, Japan

(Received 25 December 2006; accepted 21 February 2007; published online 26 March 2007)

It has been evidenced by both theory and experiments that a barrier possessing a high permittivity can create a high energy for dielectric barrier discharge. However, this argument was challenged by the recent experiments of the authors. They found an optimum permittivity value to generate denser and stronger microdischarges, as well as a high reactivity of destruction CO_2 in the entire gap space for plasma chemistry. When the barrier permittivity was higher than this optimum value, the microdischarges became sparser and even extinguished since the large number of charges resulted from higher permittivity accumulated on the dielectric surface to reduce the electric field.
 [DOI: 10.1063/1.2716848]

Any success in research and development of a feasible CO_2 utilization will signify the attainment of double objectives of slowing down a buildup of greenhouse gases in the atmosphere and better carbon resource recycling utilization. Many investigations have been done, and a nonequilibrium plasma rout is one of the most promising methods, including corona discharge by a packed-bed reactor,[1] dielectric barrier discharge (DBD) plasma,[2,3] etc., to depend on some dielectric materials for both cases. However, a high permittivity dielectric ceramic generally exhibits low fracture and low dielectric strengths so that it tends to break down under a strong current pulse in a DBD apparatus, although a high permittivity can theoretically create a high energy.[4] We have developed a dielectric barrier material, $Ca_{1-x}Sr_xTiO_3$ with $Li_2Si_2O_5$ additive, which has a high relative density, a high dielectric constant, and a high dielectric strength.[5–7] This ceramic was used as dielectric barriers to ignite dense and strong plasma with high energy.[5] Moreover, it was employed to break down CO_2 efficiently by a DBD plasma.[6,7] Comparative studies showed that the CO_2 reactivity increased with increasing relative permittivity of the barrier materials and both of them followed the sequence $Ca_{1-x}Sr_xTiO_3 \geqslant$ alumina $(Al_2O_3) \geqslant$ silica glass (SiO_2).[6,7] However, our recent in-depth study showed an existence of an optimum permittivity for the barrier materials to generate dense and strong current pulses.

$Li_2Si_2O_5$ was prepared by a conventional solid state reaction using powders of Li_2CO_3 and amorphous SiO_2. They were mixed, calcined, and remilled with zirconia balls in a polyethylene bottle. $CaTiO_3$, $SrTiO_3$, and $BaTiO_3$ powders were supplied by the Sakai Chemical Industry Co. Appropriate quantities of $CaTiO_3$, $SrTiO_3$, $BaTiO_3$, and $Li_2Si_2O_5$ were wet mixed with ZrO_2 balls and ethanol. The mixtures were dried and then ground by an agate mortar. The specimens were pressed uniaxially at 20 MPa and cold isostatically at 200 MPa, and then sintered in air. The sintered bodies were sliced and ground to be used as the dielectric barriers. The permittivity was measured by an impedance analyzer (Agilent Tech., 4299A) using a pellet sample of 6 mm in diameter and 5 mm in thickness.

The experimental setup for the CO_2 decomposition is shown in Fig. 1. A planar DBD plasma reactor, whose shell was made of Teflon, was used for CO_2 decomposition. The fictitious gas mixture $(CO_2:N_2=10:90)$ was fed into two parallel-plate electrodes $(24\times12\times3\ mm^3)$ made of stainless steel at a flow rate of 100 ml/min, where the ground electrode was covered with a 1 mm thick dielectric barrier $(30\times15\ mm^2)$. The gap space between the dielectric barrier and the counterelectrode (high-voltage electrode) was 1 mm, and the CO_2 destruction was carried out under atmospheric pressure by using a conventional flow system. The CO_2 concentration was quantitatively analyzed by a CO_2 meter (Shimadzu URA107). A sinusoidal voltage was applied to the electrodes by an ac high-voltage amplifier with a function generator (Trek 12193). A current probe (Iwatsu SS-240) with about 15 A peak and 0.1 V/A was employed. The applied voltage was increased stepwise with 1 kV/min in time until the plasma was generated and then was held at this discharge onset voltage. During the plasma generation, the discharge processes were continuously monitored by a multichannel digital oscilloscope (Iwasaki DS-8812).

Characteristics of DBD plasmas generated by various dielectric barriers with different permittivities are shown in Fig. 2, where the sinusoidal curve represents the voltage applied to the electrodes to generate the plasma. It may be found that the sinusoidal profiles were changed from smooth

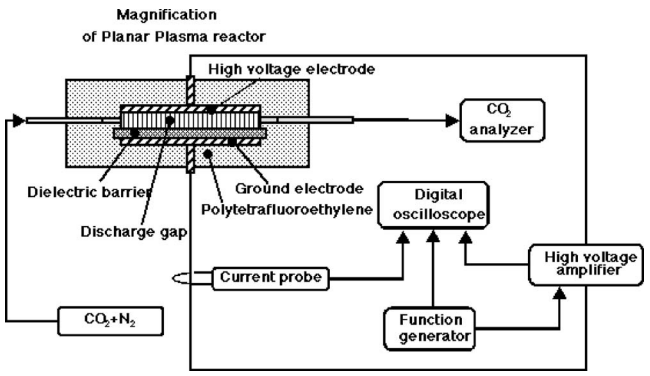

FIG. 1. Schematic diagram of experimental apparatus.

[a]Author to whom correspondence should be addressed. Electronic mail: ruixingli@yahoo.com
[b]Permanent address: Institute of Process Engineering, Chinese Academy of Sciences.

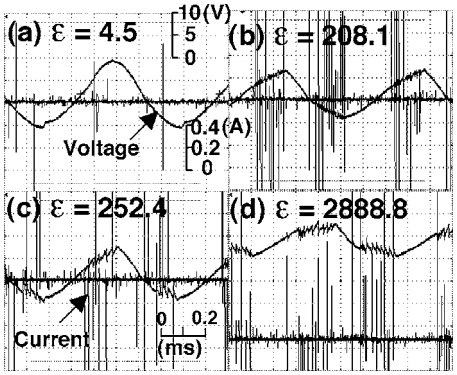

FIG. 2. Profiles of microdischarges using barriers of (a) commercial silica glass, and as-prepared (b) $Ca_{0.8}Sr_{0.2}TiO_3$ and (c) $Ca_{0.6}Sr_{0.4}TiO_3$ with 0.5 wt % $Li_2Si_2O_5$ sintered at 1200 °C for 2 h and (d) $BaTiO_3$ with 1.5 wt % $Li_2Si_2O_5$ sintered at 1100 °C for 15 min at an input ac frequency of 2 kHz (permittivity ε: 25 °C and 10 MHz).

ones [Figs. 2(a) and 2(b)] to zigzaglike ones [Figs. 2(c) and 2(d)] with increasing the permittivities of the barriers. The microdischarges became sparser and even extinguished when clear and deep zigzaglike profiles were exhibited. Additionally, it could be found that those zigzags always tended to decrease the voltage value. That is to say, the ac voltage of the reactor was not stable and tended to drop during the burst process of the DBD plasma. This might be attributed to the large number of charges resulted from the higher permittivity of the barriers accumulated on the dielectric surface to reduce the electric field.[8] The key factor, here, is the decrease of the reactor voltage. It is known that the plasma may be generated just because the voltage is higher than the discharge onset voltage of the background gas. Otherwise, a current pulse will choke as soon as the voltage is lower than this onset voltage. This is why sparser and even extinguished current pulses are exhibited in Figs. 2(c) and 2(d).

It is known that dielectric barrier serves two functions:[4,8] it limits the amount of charge transported by a single microdischarge and distributes the microdischarges over the entire electrode/barrier area. If the electric field in the gas gap is sufficiently high to initiate avalanches, microdischarges are established simultaneously and surface discharges described above cover the dielectric barrier. As long as the external sinusoidal voltage is rising, additional microdischarges will occur at new positions because the presence of residual charges on the surface of dielectric has reduced the electric fields at the positions where microdischarges have already occurred. Generally, this process goes along circularly to generate more and more filament discharges until the voltage is reversed. However, there were too much residual charges on the surface of dielectric barrier so that a great decrease of the electric fields was caused and a compensation of this downturn by external voltage to exceed the discharge onset voltage needed time to generate new microdischarges. Thus, the amount of microdischarges was limited and could not distribute on the entire barrier surface if the permittivity of the barrier was too high. Additionally, the residual channels of the extinguished microdischarges remain in the gap if the channels have not recovered sufficiently in the meantime. Otherwise, they tend to disappear. These residual channels represent privileged locations for the ignition of new microdischarges, if the applied voltage is reversed. At this time, the voltage across the gas is dominated by the memory

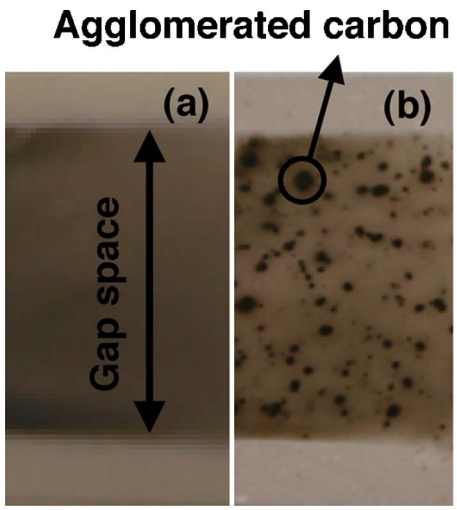

FIG. 3. (Color online) Photographs of carbon deposition on the surfaces of (a) $Ca_{0.8}Sr_{0.2}TiO_3$ (ε=208.1) and (b) $Ca_{0.6}Sr_{0.4}TiO_3$ (ε=252.4) dielectric barriers after a CO_2 destruction plasma reaction (permittivity ε: 25 °C and 10 MHz).

charges deposited on the surface and new microdischarges of opposite polarity occur. These discharges prefer the residual channels of previous microdischarges. Consequently, the less residual channels, the less microdischarges of opposite polarity were ignited. On the other hand, from a perspective of plasma chemistry, each individual microdischarge can be regarded as a miniature reactor. Thus, the plasma reactions were only limited at the positions of channels and could not distribute the entire gap space due to the difficulty of developing new microdischarges after the old channels choked if the barrier permittivity was too high. This argument is more pronounced by observing the behavior of carbon deposition accompanied with the CO_2 conversion in Fig. 3. Carbon powders uniformly deposited on the surface of the $Ca_{0.8}Sr_{0.2}TiO_3$ barrier with a permittivity of 208.1 [Fig. 3(a)], whereas an obvious agglomeration was exhibited when $Ca_{0.6}Sr_{0.4}TiO_3$ barrier with a permittivity of 252.4 was used [Fig. 3(b)]. The nonuniform accumulation of carbon powder might be attributable to a heterogeneous reaction related to

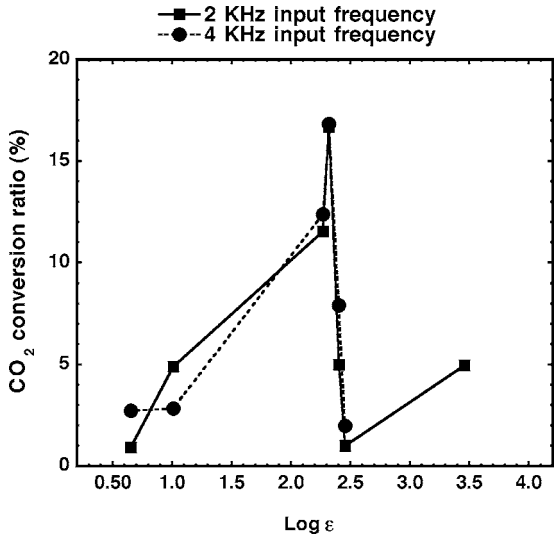

FIG. 4. Logarithmic permittivity ε dependence of CO_2 conversion using commercial silica glass and alumina, as-prepared $Ca_{1-x}Sr_xTiO_3$ ($0.1 \leqslant x \leqslant 1$), and $BaTiO_3$ dielectric barriers.

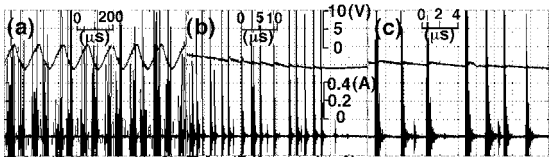

FIG. 5. Various magnified profiles of microdischarges using the dielectric barrier of as-prepared $Ca_{0.8}Sr_{0.2}TiO_3$ with 0.5 wt % $Li_2Si_2O_5$ (ε=208.1 at 25 °C and 10 MHz) sintered at 1200 °C for 2 h at an input ac frequency of 8 kHz.

the limitation of microdischarge channels. Furthermore, the ability of CO_2 destruction was decreased with increasing the permittivity of the barrier after achieving a maximum CO_2 conversion, as shown in Fig. 4. This is another evidence of less microdischarge channels by a high permittivity barrier in the gap space. The optimum value of the permittivity was around 208 (measured at 25 °C and 10 MHz), i.e., the barrier of $Ca_{0.8}Sr_{0.2}TiO_3$, at input reactor frequency between 2 and 4 kHz. The characteristics of the current pulse caused by $Ca_{0.8}Sr_{0.2}TiO_3$ at ac frequency of 8 kHz are shown in Fig. 5, and it may be concluded that each pulse width was about 1 μs.

Additionally, the fraction of CO_2 conversion utilizes unit plasma power is an important parameter for a plasma chemistry. It is known that the average plasma power P is given by[4]

$$P = 4fC_D^2(C_D + C_g)^{-1}V_{\min}(V_{\max} - V_{\min}), \quad V_{\max} \geqslant V_{\min}, \tag{1}$$

where f is the applied frequency, C_D is the capacitance of the dielectric, C_g is the capacitance of the discharge gap, $V_{\min}$ is the minimum external voltage required to maintain a discharge, and $V_{\max}$ is the maximum value of the applied sinusoidal voltage wave. Furthermore, the capacitance C is given by

$$C = \varepsilon_0 \varepsilon S/d, \tag{2}$$

where $\varepsilon_0 = 8.85 \times 10^{-12}$ F/m, ε is the relative permittivity, and S and d are the area of the electrode and the distance between two parallel-plate electrodes, i.e., either 1 mm gap of air or 1 mm thickness of the barrier in the present study, respectively. The efficiency of CO_2 decomposition was defined as

$$\text{Efficiency}(\%/W) = \text{CO}_2\text{conversion}(\%)/P(W) \times 100\,\%\,, \tag{3}$$

where P is the plasma energy calculated by Eq. (1). As shown in Fig. 6, the efficiency is not very high for the $Ca_{0.8}Sr_{0.2}TiO_3$ barrier with a high permittivity. This is probably attributed to plentiful "hot" electrons could dissociate both forward and reverse reactions in the gap space.

Consequently, from the present results, it seems that there is an optimum permittivity of the barrier material for generation of dense and strong DBD plasma. The CO_2 conversion attained to maximum by DBD plasma at input ac frequency between 2 and 4 kHz when $Ca_{0.8}Sr_{0.2}TiO_3$ with permittivity of 208 (25 °C and 10 MHz) was used as a barrier material. On the other hand, when $Ca_{0.6}Sr_{0.4}TiO_3$ and $BaTiO_3$ that possessed higher permittivities were used as the barrier materials, nonuniform microdischarge channels tended to occur so that the chemical reaction was not able to take place in the entire gap space to cause a decrease of reaction ability.

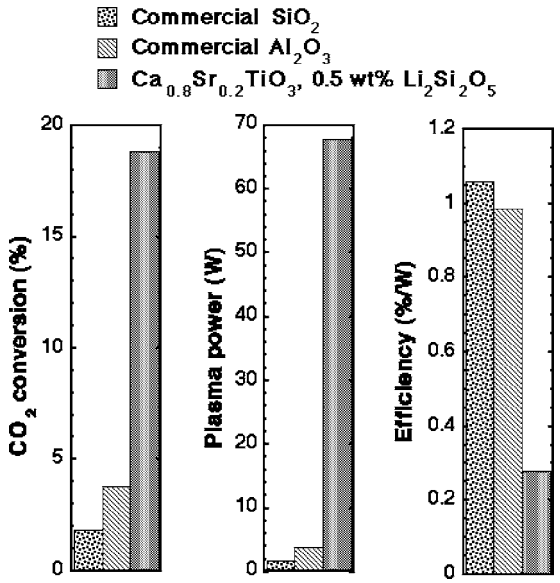

FIG. 6. Plasma energy and efficiency for as-prepared $Ca_{0.8}Sr_{0.2}TiO_3$ with 0.5 wt % $Li_2Si_2O_5$ (ε=208.1), commercial alumina (ε=10.3), and silica glass (ε=4.5) (permittivity ε: 25 °C and 10 MHz).

This research was carried out as one of the projects in the MSTEC Research Center at IMRAM, Tohoku University. It was partially supported by the JSPS Asian Core Program "Interdisciplinary Science of Nanomaterials." The authors are indebted to B. Liu in the IMRAM, Tohoku University for his help rendered in photography and the management of the Sakai Chemical Industry Co. for supplying the starting powders of $CaTiO_3$, $SrTiO_3$, and $BaTiO_3$ used in the present study.

[1]K. Jogan, A. Mizuno, T. Yamamoto, and J. Chang, IEEE Trans. Ind. Appl. **29**, 876 (1993).
[2]G. Zheng, J. Jiang, Y. Wu, R. Zhang, and H. Hou, Plasma Chem. Plasma Process. **23**, 59 (2003).
[3]S. L. Suib, S. L. Brock, M. Marquez, J. Luo, H. Matsumoto, and Y. Hayashi, J. Phys. Chem. B **102**, 9661 (1998).
[4]U. Kogelschatz, Plasma Chem. Plasma Process. **23**, 1 (2003).
[5]R. Li, Q. Tang, S. Yin, Y. Yamaguchi, and T. Sato, Phys. Plasmas **11**, 3715 (2004).
[6]R. Li, Q. Tang, S. Yin, and T. Sato, Plasma Chem. Plasma Process. **26**, 267 (2006).
[7]R. Li, Q. Tang, S. Yin, and T. Sato, Fuel Process. Technol. **87**, 617 (2006).
[8]*Low Temperature Plasma Physics*, edited by R. Hippler, S. Pfau, M. Schmidt, and K. H. Schoenbach (Wiley-VCH, Berlin, 2001).